

See discussions, stats, and author profiles for this publication at: <https://www.researchgate.net/publication/358670643>

Biominerals in the leaves of Agave karwinskii Zucc

Article in *Results in Chemistry* · February 2022

DOI: 10.1016/j.rechem.2022.100309

CITATION

1

READS

103

3 authors, including:



Margarita Mondragon

Instituto Politécnico Nacional

36 PUBLICATIONS 592 CITATIONS

[SEE PROFILE](#)



Biominerals in the leaves of *Agave karwinskii* Zucc

Margarita Mondragón ^{a,*}, Luis E. Elizalde ^b, Victor Rejón ^c

^a Instituto Politécnico Nacional (IPN), CIIDIR-Oaxaca, C. Hornos 1003, 71230 Santa Cruz Xoxocotlán, Oax., Mexico

^b Centro de Investigación en Química Aplicada (CIQA), Enrique Reyna H. 140, 25294 Saltillo, Coah., Mexico

^c CINVESTAV-LANNBIO, Km. 6 Carr. Mérida - Progreso, 97205 Mérida, Yuc., Mexico

ARTICLE INFO

Keywords:

Agave karwinskii

Biominerals

Calcium carbonate

Chantalite

ABSTRACT

The leaves of two ethnotaxa of *Agave karwinskii* Zucc., ‘Cuishe’ and ‘Madrecuishe’, were analyzed using field emission scanning electron microscopy (FE-SEM) with energy dispersive X-ray spectroscopy (EDX), X-ray diffraction (XRD), and Fourier transform infrared spectroscopy (FTIR) to characterize their occurring biominerals. The sharp and high peak at 20 21.4° in the XRD patterns and the prominent bands’ envelopes related to aluminosilicates in the FTIR spectra showed the occurrence of chandalite in the leaves of both ethnotaxa. For the first time, chandalite is reported as a biomineral occurring naturally in *Agave* plants. The FE-SEM/EDX results revealed needle-shaped calcium oxalate profusely dispersed near the upper epidermis, in addition to uncovering the presence of calcium carbonate and silica in particles of irregular shape. Intriguingly, the occurrence of both minerals in *Agave* plants has not been reported either, suggesting complex biomineralization patterns in *Agave karwinskii*. It is proposed that calcium carbonate in the leaves of *Agave* is formed by the reaction of chandalite with CO₂.

Introduction

The formation of both crystalline and amorphous composite mineral phases by biological organisms has received increasing attention [1–3]. To date, numerous studies have largely focused on primarily amorphous hydrated silica (SiO₂), as well as calcium oxalate (CaOx) crystals and calcium carbonate (CaCO₃) in the form of cystoliths [4–11].

CaOx crystals are the most common type of biominerals found in plants, accounting for 3%–80% of a plant’s dry weight and as much as 90% of its total calcium content [4]. Although their function in normal plant growth and development remains unclear, they could represent a form of stored calcium and oxalate acid. Likewise, the formation of CaCO₃ is another component of calcium metabolism but one that is less responsive to changes in calcium supply [5].

In stark contrast, Si amounts to just ca. 0.1%–10% of plant dry weight. Yet, without Si, plants are often weaker structurally and more prone to abnormalities in growth and reproduction [12–14]. Plants take up silicon from soil water in the form of water-soluble Si(OH)₄ or Si(OH)₃O₂, which is then polymerized and precipitated as amorphous hydrate silica (SiO₂ with 5%–15% H₂O) [15].

The role of CaOx crystals, CaO₃, and SiO₂ in metal detoxification by plants has also been explored [4,16–18]. Studies of plants sensitive to Al

and some heavy metals have revealed that CaOx crystals may or may not incorporate them into their structure, depending on both the metal element in question and plant species identity [4,16]. Some reports on CaCO₃ have found evidence for the sequestration of heavy metals, such as manganese, zinc, and strontium [16]. Further, the coprecipitation of aluminum and heavy metals with silicon in the cell walls contribute to the alleviation of their toxicity to plants [16–18].

Although abundant calcium oxalate (CaOx) crystals were reported in leaves of several species of *Agave* (Agavaceae), such studies are still lacking for *Agave karwinskii* Zucc [19–22]. *Agave* plants are keystone species in semiarid to arid regions whose geographic center of origin is Mexico, but whose populations have since spread and now range from southwestern U.S. through Central America, the Caribbean, and into northern South America [23]. To the authors’ best knowledge, neither the presence of SiO₂ nor CaCO₃ has yet been explored in *A. karwinskii*, much less any other *Agave* species. Accordingly, the aim of this work was twofold. First, to study the morphology of CaOx crystals in leaves of two ethnotaxa of *A. karwinskii*: ‘Cuiche’ and ‘Madrecuishe’, and second, to determine if CaCO₃ and SiO₂ are present in *A. karwinskii* leaves. Mineral nutrients are among the main environmental factors affecting plants’ development, physiology, and metabolism. Given that the vegetative to inflorescence transition in most *Agave* species occurs between 8 and 12

* Corresponding author.

E-mail address: mmondragon@ipn.mx (M. Mondragón).

years after their planting, which signals maturity and their imminent death, we used *Agave* plants ca. 8 years old [24,25].

Material and methods

Two independent adult plants of each ethnotaxa ‘Cuishe’ and ‘Madrecuishe’ were selected from a plantation in the community of El Nanche ($96^{\circ}33'29.000''$ S, $16^{\circ}24'24.999''$ E; elevation: 1520 m a.s.l.), located in the district of Miahuatlán of Porfirio Díaz, Oaxaca State, Mexico. Three slices rectangular in shape ($\sim 1.5 \text{ cm} \times 2 \text{ cm}$) were cut in the field, from the central section of two middle leaves of each plant. They were immediately fixed in a solution of formalin, glacial acetic acid, ethanol (95%), and deionized water (10:5:50:35) for 48 h, after which each sample was washed with deionized water and dehydrated in an ethanol series [26].

Wafer-thin slices of the transverse rectangular sections were cut with a razor, allowed to dry, and then pressed between two glass slides to preserve them plain. Next, their surfaces were examined under a field emission scanning electron microscope (FE-SEM, JEOL JSM-7600F), and their elemental analysis performed by energy dispersive X-ray (EDX) spectroscopy.

The presence of crystalline phases in the ground leaves of ‘Cuishe’ and ‘Madrecuishe’ was assessed by X-ray diffraction (XRD) (Bruker D8 Advance XRD, Cu K α radiation, $2\theta = 10\text{--}80^\circ$, scan of 0.02° per step, scan rate of $0.5 \text{ s}/\text{step}$). Infrared spectra of the ground samples in the spectral range spanning 4000 and 400 cm^{-1} were recorded on a Nicolet iS10 FTIR spectrophotometer, using two different modes (i.e., ATR and KBr pellets).

Results and discussion

SEM-EDX analysis

For both ethnotaxa, ‘Cuishe’ and ‘Madrecuishe’, representative SEM images of thin transverse sections of their leaves showed needle-like raphide crystals profusely dispersed near the upper epidermis (Fig. 1). Their corresponding EDX elemental mapping of calcium corroborated the inference that Ca is heavily deposited in these crystals (insets in Fig. 1). A preponderance of raphide-calcium oxalate crystals with pointed ends has been reported for other *Agave* species (*A. tequilana*, *A. americana*) [19–21]; however, all three druses-, raphides- and styloids-oxalate crystals were identified in *A. atroviridis* [22]. Calcium oxalate crystals form and location are generally a species-specific trait [27].

It is noteworthy that only a few of these crystals were observed towards the center of the mesophyll and near the lower epidermis of the leaf (Fig. 2), in comparison with crystals common near the upper epidermis. This finding supports the view that calcium oxalate crystals are linked to the control of water evaporation in *Agave* plants [28].

Conversely, the EDX maps of silicon uncovered only a few bright spots (high density of dots), near the upper epidermis (Fig. S1). Both SEM and EDX analyses were focused on those regions. There, irregular bodies (on average up to $7.5\text{-}\mu\text{m}$ long and $5\text{-}\mu\text{m}$ wide) were found in ‘Cuishe’ and ‘Madrecuishe’ leaves (Fig. 3a–d). Their EDX spectra indicated the presence not only of Si and O but also Al and Ca. Table 1 summarizes the surface elemental composition of the bodies shown in Fig. 3a–d. The Si, Al, and Ca content could reach up to 18.22 wt%, 7.13 wt%, and 4.09 wt%, respectively. The content of Mg was less than 1 wt %, while all other metals occurred in insignificant quantities.

X-Ray diffraction analysis

Through an analysis of their X-ray diffractograms, it was verified that the major crystalline phases present in ground *Agave* leaves of both ethnotaxa are calcium oxalate monohydrate ($\text{CaC}_2\text{O}_4\cdot\text{H}_2\text{O}$, whewellite [w]) and cellulose [c] (Fig. 4).

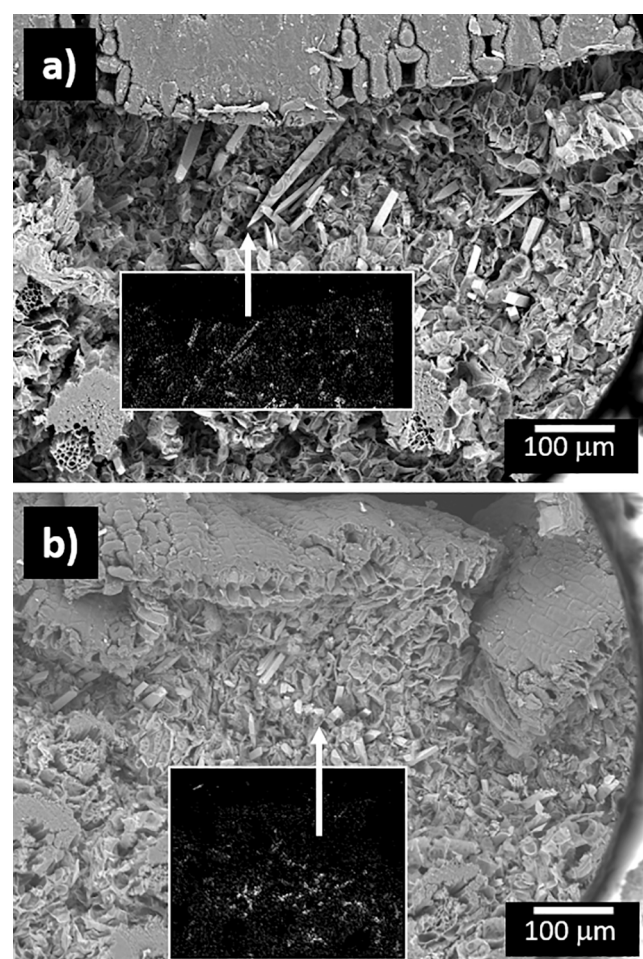


Fig. 1. Transversal section of leaves of *A. karwinskii*, near upper epidermis: a ‘Cuishe’, and b) ‘Madrecuishe’.

The sharp diffraction peaks at $2\theta 14.9^\circ$, 15.2° , 24.3° , 30.1° , 31.4° , 38.3° and 46.9° correspond to calcium oxalate, in accordance with the JCPDS card no. 00-020-0231. The other small peaks between them also correspond to CaOx. Cellulose is the main component of *Agave* leaves, these having low amounts of lignin and hemicellulose and a diverse range of non-cellulosic polysaccharides [29]. The diffraction peak at $2\theta \sim 22.7^\circ$ was assigned to cellulose type I [30]. The other characteristic diffraction bands of cellulose type I at $2\theta 14.7^\circ$ and 16.8° were superimposed on the 14.9° and 15.1° bands of the CaOx, and were not clearly distinguishable. Further, the undefined band in the 2θ -range of $\sim 15^\circ\text{--}30^\circ$, which is usually related to amorphous biogenic SiO_2 , could be superimposed with the amorphous component of cellulose, making it difficult to assess its presence by X-ray diffractometry alone.

An interesting feature was the sharp and high peak at $2\theta 21.4^\circ$, located a bit lower than the diffraction peak of cellulose at $2\theta 22.7^\circ$. Automated phase identification from the XRD data suggested the presence of chandalite ($\text{CaAl}_2\text{SiO}_4(\text{OH})_4$), a natural calcium aluminum silicate. The diffraction peaks at $2\theta 21.3^\circ$ and 15.3° assigned to this phase (JCPDS card no. 01-083-1450) could be superimposed on the diffraction peaks of cellulose or calcium oxalate around these positions. Published reports on biominerals present in Cactaceae species have documented complex biominerization patterns, revealing some other biominerals besides calcium oxalate (either monohydrated or dihydrated), such as biogenic amorphous SiO_2 , α -quartz, calcite (CaCO_3), and even gushkinsite, a dihydrated magnesium oxalate ($\text{MgC}_2\text{O}_4 \cdot 2\text{H}_2\text{O}$) [31,32]. Agaves and cacti plants are remarkably similar physiologically: both conserve water and can cope with aspects of climate change, including increasing atmospheric CO_2 levels, rising temperatures, and changing

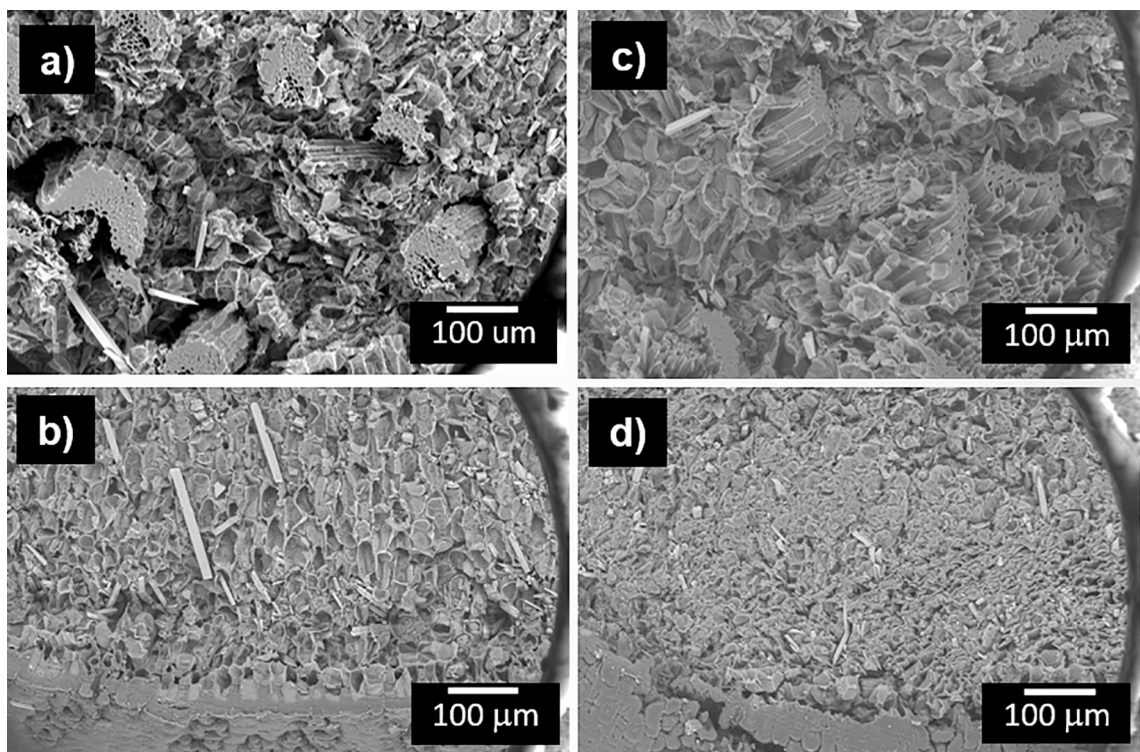


Fig. 2. SEM images of transversal section of leaves. ‘Cuishe’: a) in the middle of mesophyll, and b) near lower epidermis. ‘Madrecuishe’: c) in the middle of mesophyll, and d) near lower epidermis.

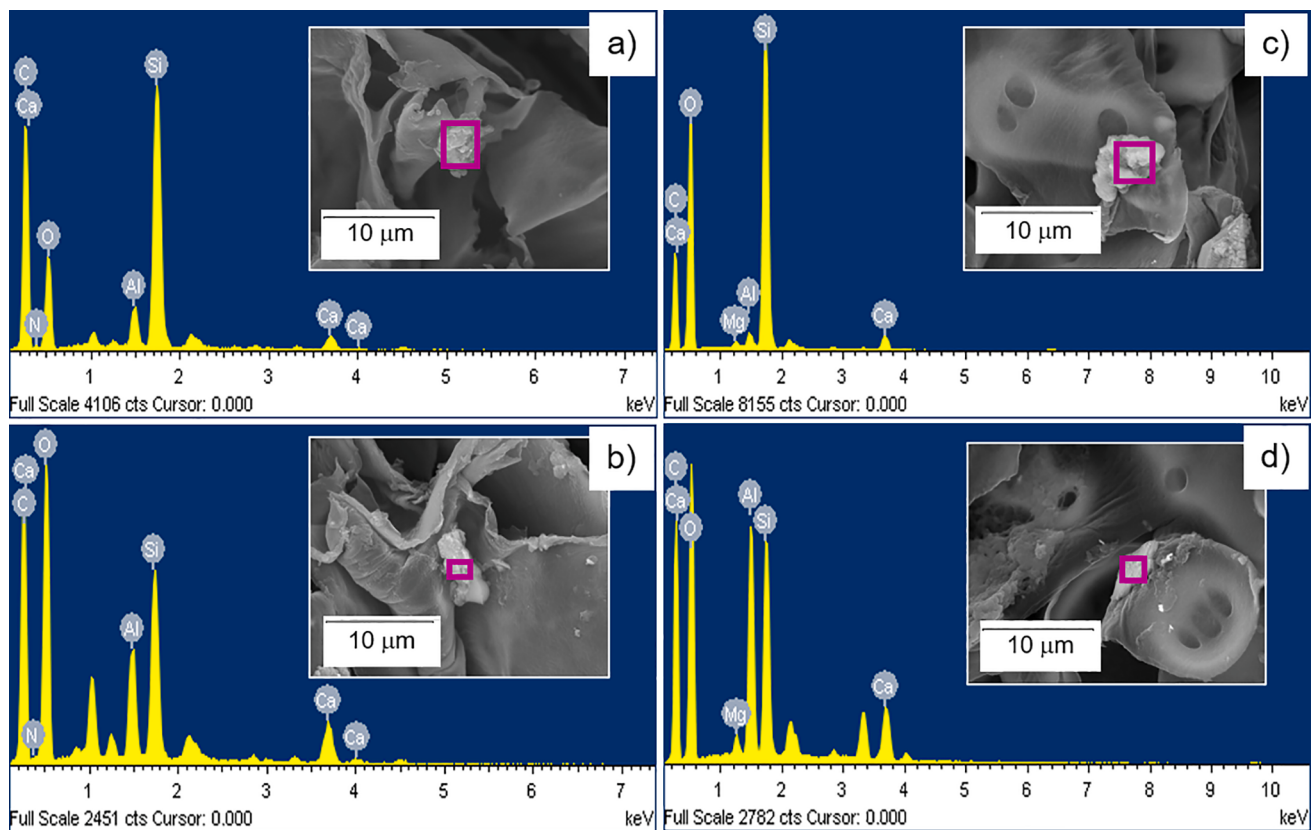


Fig. 3. EDX spectra of particles detected by Si maps (insets represent their SEM images) of: a) and b) ‘Cuishe’ leaves; c) and d) ‘Madrecuishe’ leaves.

Table 1

Surface elemental composition of particles in leaves of both ethnotaxa of *A. karwinskii* by EDX analysis.

Element wt. %	a)	b)	c)	d)
C	57.06	41.71	32.63	38.97
O	24.27	39.32	46.35	41.30
Si	12.87	6.42	18.22	7.97
Al	1.63	3.40	0.62	7.13
Ca	1.60	2.83	1.88	4.09
Mg	0.22	0.77	0.31	0.55

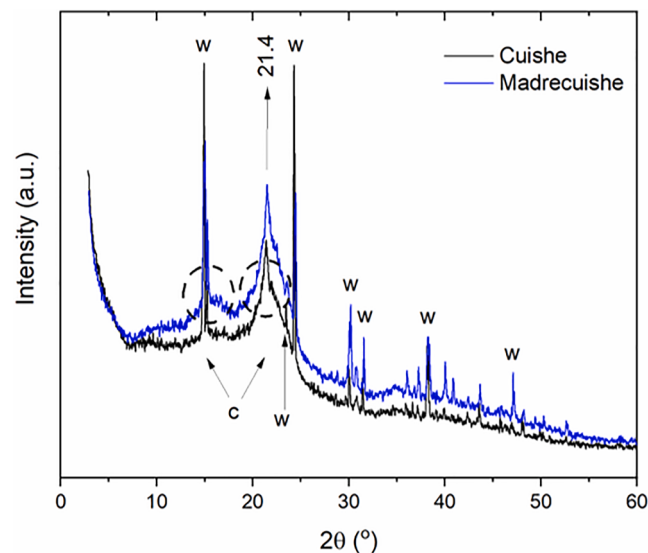


Fig. 4. X-ray diffractograms of ground leaves of the ethnotaxa of *A. karwinskii*: 'Cuishe', and 'Madrecuishe'.

rainfall patterns [33]. There are also other reports of naturally generated minerals by interactions of living organisms with the mineral surrounding [34–36]. Vibrational spectroscopy is a valuable tool for probing those structures that cannot be unambiguously determined by diffraction techniques [37]. Hence, vibrational spectral analysis was carried out here using FTIR spectroscopy.

FTIR spectroscopy analysis

The FTIR spectra of ground leaves of 'Cuishe' and 'Madrecuishe' collected in the ATR mode (range: 4000–950 cm⁻¹) are shown in Fig. 5a and Fig. 5b, respectively. Their corresponding spectra collected in KBr pellets appear in Fig. 6a and b (range: 980–400 cm⁻¹; bands in this region were better defined using KBr pellets than the ATR mode). The characteristic band of CaOx at ~ 1620 cm⁻¹, assigned to asymmetric carboxylate stretching, was superimposed on the characteristic bands of lignin at ~ 1610 cm⁻¹ and 1515 cm⁻¹, corresponding to aromatic ring vibrations, giving rise to the band covering the range of 1700–1480 cm⁻¹ [38,39]. The band at 1317 cm⁻¹ corresponding to the symmetric carboxylate stretching of the CaOx was clearly seen.

The presence of calcium carbonate (CaO₃) was confirmed by the strong band at 1416 cm⁻¹ assigned to asymmetric (ν_{3b}) stretching vibration of carbonate, and the inflection points at 875 cm⁻¹ and 720 cm⁻¹ associated with the CO₃²⁻ out-of-plane (ν_2) and in-plane (ν_4) bending. The sharp peak at 670 cm⁻¹ could be due to the component (ν_{4b}) of the band that corresponds to the normal mode ν_4 for amorphous CaCO₃ [40,41]. This was surprising, because CaOx and CaCO₃ occurring together was never reported in previous studies of *Agave*, although their combination has been found in various Cactaceae species [31]. The band spanning 912–869 cm⁻¹ was ascribed to the superimposition of the band

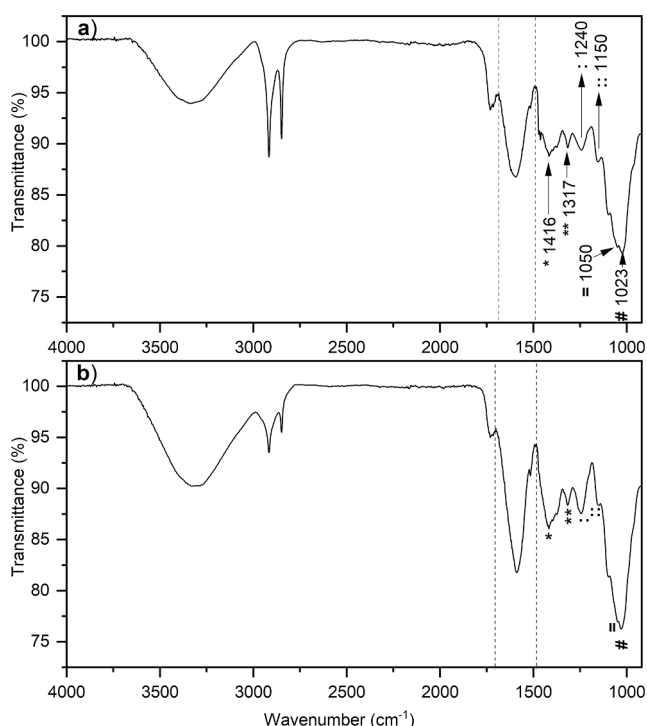


Fig. 5. FTIR spectra of ground leaves of a) 'Cuishe' and b) 'Madrecuishe' collected in the ATR mode (range: 4000–950 cm⁻¹).

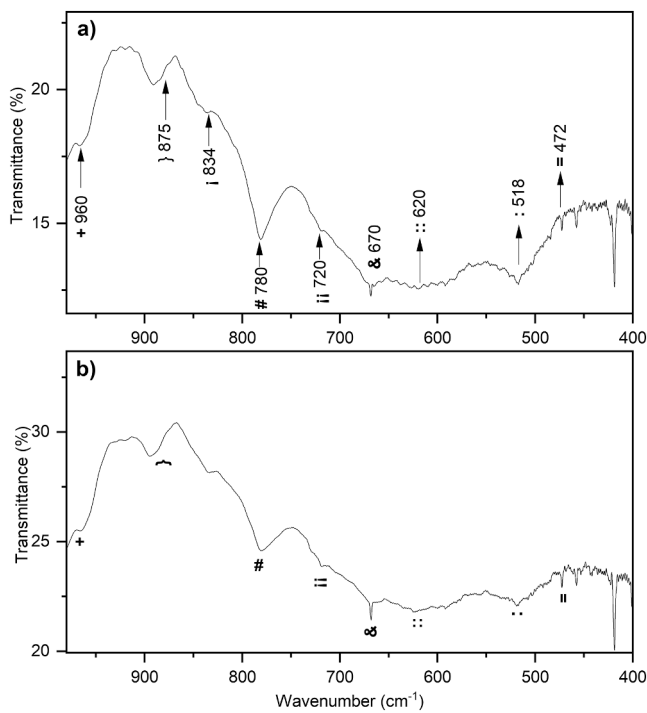


Fig. 6. FTIR spectra of ground leaves of a) 'Cuishe' and b) 'Madrecuishe' collected in KBr pellets (range: 980–400 cm⁻¹).

at 875 cm⁻¹ associated with carbonate upon that at 893 cm⁻¹ associated with the cellulosic β-glycosidic linkages between the glucose units in cellulose [42]. The formation of calcium carbonate can arise from the reaction of chalcolite with high dosages of CO₂, at least in red muds [43]. Considering that *Agave* plants can draw down and sequester large amounts of atmospheric CO₂, through natural photosynthesis, coupled

with the XRD fixation results for the leaves of both *A. karwinkii* ethno-taxa suggesting the possibility of a chandalite phase; the idea of chandalite undergoing transformation to further obtain calcium carbonate is plausible. The possibility of hydroxyaluminosilicates formed by the interaction of silicic acid with aqueous aluminum has already been posited [44]. Therefore, the FTIR spectra were scanned further, to find the prominent band envelopes known to characterize silicate and aluminosilicate [45].

These identified bands were as follows: (a) The band due to asymmetric stretching vibration of Si-O-Si or Si-O-Al connected with the tetrahedron of $[\text{SiO}_4]$ or $[\text{AlO}_4]^-$ was observed in the region of $867\text{--}1190\text{ cm}^{-1}$ (respectively at 1050 cm^{-1} or 1023 cm^{-1}) [46]. Both longitudinal optical (LO_2 and LO_1) modes that generally accompany the Si-O-Si asymmetric stretching mode can be seen at 1150 cm^{-1} and 1240 cm^{-1} [47]. The inflection point detected around 960 cm^{-1} was identified as $(\text{Si}, \text{Al})\text{-O}\text{-}(\text{H} \cdot \cdot \text{H}_2\text{O})$, whereas the band associated with the bending mode of $(\text{Si}, \text{Al})\text{-O}$ was noted at 472 cm^{-1} [48,49]. (b) The symmetric stretching vibration between Si-O-(Si, Al) in the tetrahedron of $[\text{SiO}_4]$ or $[\text{AlO}_4]^-$ was observed at 780 cm^{-1} [46]. This contrasts with the Si-O-Si symmetric stretching mode for vitreous silica reported at 800 cm^{-1} [50]. (c) Also of pertinent interest is the presence of bands related to transition aluminas [45,51]. These wide bands peaked at 518 cm^{-1} and 620 cm^{-1} were related to octahedrally (AlO_6) coordinated aluminum, while the inflection points at 720 cm^{-1} and 834 cm^{-1} were related to tetrahedrally (AlO_4) coordinated aluminum. Altogether, these results are consistent with the presence of chandalite in leaves, which could lead to the formation of calcium carbonate due to its reaction with CO_2 , as previously stated. Chandalite structure consists of CaO_8 , AlO_6 and SiO_4 polyhedra [52].

We should not overlook the broad band observed in the hydroxyl stretching region, covering the range of $\sim 2990\text{--}3660\text{ cm}^{-1}$. It is likely related to asymmetric stretching and bending vibrations of Si-OH stretching mode, or to the free O-H stretching vibration of the OH group in cellulose, or both [53].

Conclusions

Combined X-ray diffraction and FTIR spectroscopy were shown to be very useful for studying the biominerals present in the leaves of *Agave karwinskii* Zucc. For the first time, the presence of chandalite ($\text{CaAl}_2\text{SiO}_4(\text{OH})_4$), a complex natural calcium aluminum silicate, was assessed using these two different techniques. In addition, combined FESEM/EDX and FTIR analysis revealed not only the presence of calcium oxalate crystals with pointed ends in the upper epidermis but also confirmed the presence of both calcium carbonate and silica occurring together, which was never reported in previous studies of *Agave*. We postulate that CaCO_3 is formed by the reaction of chandalite with high dosages of CO_2 . The findings presented here for *A. karwinskii* merit further examination in relation to the evolved biominerization patterns in the *Agave* genus.

CRediT authorship contribution statement

Margarita Mondragón: Conceptualization, Investigation, Supervision. **Luis E. Elizalde:** Investigation, Visualization. **Victor Rejón:** Investigation, Writing – review & editing.

Declaration of Competing Interest

The authors declare that they have no known competing financial interests or personal relationships that could have appeared to influence the work reported in this paper.

Acknowledgements

The authors would like to acknowledge Dra. P. Quintana (CINVESTAV Mérida-IPN) the access to the National Laboratory of Nano and

Biomaterials (LANNBIO: FOMIX-Yucatán 2008-108160, CONACYT LAB-2009-01-123913, 292692, 294643, 188345, 204822) and to MSc. D. Aguilar-Treviño the acquisition of diffraction patterns. This work was supported by the Research and Postgraduate Secretary (SIP) of IPN [grant number SIP 20211514].

Appendix A. Supplementary data

Supplementary data to this article can be found online at <https://doi.org/10.1016/j.rechem.2022.100309>.

References

- [1] A. Sugawara-Narutaki, J. Nakamura, C. Ohtsuki, Polymer-induced liquid precursors (PILPs) and bone regeneration, in: A. Osaka, R. Narayan (Eds.), *Bioceramics: From Macro to Nanoscale*, Elsevier Ltd, New York, 2021, pp. 391–398.
- [2] G.M. Khalifa, K. Kahil, L. Addadi, S. Weiner, Calcium ion and mineral pathways in biominerization: A perspective, in: K. Endo, T. Kogure, H. Nagasawa (Eds.), *Biominerization: From Molecular and Nano-structural Analyses to Environmental Science*, Springer Open, 2018, pp. 97–104.
- [3] H.C.W. Skinner, H. Ehrlich, Biominerization, in: K. Turekian, H. Holland (Eds.), *Treatise on Geochemistry*, Elsevier Ltd, New York, 2014, pp. 106–162.
- [4] V.R. Franceschi, P.A. Nakata, Calcium oxalate in plants: Formation and function, *Annu. Rev. Plant Biol.* 56 (1) (2005) 41–71, <https://doi.org/10.1146/annurev.aplant.56.032604.144106>.
- [5] C.C. Wu, S.J. Chen, T.B. Yen, L.L. Kuo-Huang, Influence of calcium availability on deposition of calcium carbonate and calcium oxalate crystals in the idioblasts of *Morus australis* Poir., *Leaves Bot Stud* 47 (2006) 119–127.
- [6] E.J. Baran, P.V. Monje, Oxalate biominerals, in: A. Siegel, H. Siegel, R.K.O. Siegel (Eds.), *Biominerization: From Nature to Application*, John Wiley & Sons Ltd, Chichester, 2008, pp. 219–254.
- [7] I. Nitta, A. Kida, Y. Fujibayashi, H. Katayama, Y. Sugimura, Calcium carbonate deposition in a cell wall sac formed in mulberry idioblasts, *Protoplasma* 228 (4) (2006) 201–208, <https://doi.org/10.1007/s00709-006-0182-2>.
- [8] H. He, T.M. Bleby, E.J. Veneklaas, H. Lambers, J. Kuo, Morphologies and elemental compositions of calcium crystals in phyllodes and branchlets of *Acacia seboeum* (Leguminosae: Mimosoideae), *Ann. Bot.* 109 (2012) 887–896. <https://doi.org/10.1093/aob/mcs004>.
- [9] M.A. Nawaz, A.M. Zakharenko, I.V. Zemchenko, M.S. Haider, M.A. Ali, M. Imtiaz, G. Chung, A. Tsatsakis, S. Sun, K.S. Golokhvast, Phytolith formation in plants: from soil to cell, *Plants* 8 (2019) 249, <https://doi.org/10.3390/plants8080249>.
- [10] A. McSheik, S. Cassaignon, J. Livage, A. Gibaud, S. Berthier, P.J. Lopez, Optical properties of nanostructured silica structures from marine organisms, *Front. Mar. Sci.* 5 (2018) 123, <https://doi.org/10.3389/fmars.2018.00123>.
- [11] M. Sahebi, M.M. Hanafi, A. Siti Nor Akmar, M.Y. Raffi, P. Azizi, F.F. Tengoua, J. Nurul Mayzaitul Azwa, M. Shabanimofrad, Importance of silicon and mechanisms of Biosilica formation in plants, *Biomed Res. Int.* 2015 (2015) 1–16, <https://doi.org/10.1155/2015/396010>.
- [12] J. Ma, E. Takahashi, Effect of silicon on the growth and phosphorus uptake of rice, *Plant Soil* 126 (1990) 115–119. <http://www.jstor.org/stable/42938590>.
- [13] M.J. Hodson, P.J. White, A. Mead, M.R. Broadly, Phylogenetic variation in the silicon composition of plants, *Ann. Bot.* 6 (2005) 1017–1046, <https://doi.org/10.1093/aob/mci255>.
- [14] H.A. Currie, C.C. Perry, Silica in plants: biological, biochemical and chemical studies, *Ann. Bot.* 100 (2007) 1383–1389, <https://doi.org/10.1093/aob/mcm247>.
- [15] V. Bansal, A. Ahmad, M. Sastry, Fungus-mediated biotransformation of amorphous silica in rice husk to nanocrystalline silica, *J. Am. Chem. Soc.* 128 (2006) 14059–14066, <https://doi.org/10.1021/ja062113+>.
- [16] H. He, E.J. Veneklaas, J. Kuo, H. Lambers, Physiological and ecological significance of biominerization in plants, *Trends Plant Sci.* 19 (3) (2014) 166–174, <https://doi.org/10.1016/j.tplants.2013.11.002>.
- [17] Y. Wang, A. Stass, W.J. Hors, Apoplastic binding of aluminum is involved in silicon-induced amelioration of aluminum toxicity in maize, *Plant Physiol.* 136 (2004) 3762–3770, <https://doi.org/10.1104/pp.104.045005>.
- [18] P. Bauer, R. Elbaum, I.M. Weiss, Calcium and silicon mineralization in land plants: transport, structure and function, *Plant Sci.* 180 (6) (2011) 746–756, <https://doi.org/10.1016/j.plantsci.2011.01.019>.
- [19] M. Lorenza-Salinas, T. Ogura, L. Soffchi, Irritant contact dermatitis caused by needle-like calcium oxalate crystals, raphides, in *Agave tequilana* among workers in tequila distilleries and agave plantations, *Contact Derm* 44 (2001) 94–96, <https://doi.org/10.1034/j.1600-0536.2001.440208.x>.
- [20] J. Wattendorff, Ultrastructure of the suberized styloid crystal cells in *Agave* leaves, *Planta* 128 (2) (1976) 163–165, <https://doi.org/10.1007/BF00390318>.
- [21] K.E. Espelie, J. Wattendorff, P.E. Kolattukudy, Composition and ultrastructure of the suberized cell wall of isolated crystal idioblasts from *Agave americana* L. leaves, *Planta* 155 (2) (1982) 166–175, <https://doi.org/10.1007/BF00392548>.
- [22] A. Bernardino-Nicanor, R. Mora-Escobedo, J.L. Montañez-Soto, S. Filardo-Kerstupp, L. González-Cruz, Microstructural differences in *Agave atrovirens* Karw leaves and pine by age effect, *Afr. J. Agric. Res.* 7 (2012) 3550–3559, <https://doi.org/10.5897/AJAR11.1185>.

- [23] S.V. Good-Avila, V. Souza, B.S. Gaut, L.E. Eguiarte, Timing and rate of speciation in *Agave* (Agavaceae), *Proc. Natl. Acad. Sci.* 103 (24) (2006) 9124–9129.
- [24] K.R. Corbin, C.S. Byrt, S. Bauer, S. DeBolt, D. Chambers, J.A.M. Holtum, G. Karem, M. Henderson, J. Lahnstein, C.T. Beahan, A. Bacic, G.B. Fincher, N.S. Betts, R. A. Burton, S.C. Davis, Prospecting for energy-rich renewable raw materials: agave leaf case study, *PLoS One* 10 (8) (2015) e0135382, <https://doi.org/10.1371/journal.pone.0135382>.
- [25] S.D.C. Delgado Sandoval, M.J. Abraham Juárez, J. Simpson, *Agave tequilana* MADS genes show novel expression patterns in meristems, developing bulbils and floral organs, *Sex. Plant Reprod.* 25 (1) (2012) 11–26, <https://doi.org/10.1007/s00497-011-0176-x>.
- [26] E. Solano, T. Terrazas, A. González-Becerril, Comparative anatomy of the stem, leaf and inflorescence basal axis of *Polianthes* L. (Asparagaceae, Agavoideae) species, *Feddes Repert* 124 (4) (2013) 105–115, <https://doi.org/10.1002/fedr.201300017>.
- [27] H.T. Horner, B.L. Wagner, Calcium oxalate formation in higher plants. In: S.R. Khan SR, editor. *Calcium Oxalate in Biological Systems*, New York: CRC Press; 1995, p. 53–72.
- [28] C.C. Wu, L.L. Kuo-Hang, Calcium crystals in the leaves of some species of Moraceae, *Bot. Bull. Acad. Sin.* 38 (1997) 97–104.
- [29] H. Li, S. Pattiathil, M.B. Foston, S.Y. Ding, R. Kumar, X. Gao, A. Mittal, J. M. Yarbrough, M.E. Himmel, A.J. Ragauskas, M.G. Hahn, C.E. Wyman, Agave proves to be a low recalcitrant lignocellulosic feedstock for biofuels production on semi-arid lands, *Biotechnol. Biofuels* 7 (2014) 50. <http://www.biotechnologyforbiofuels.com/content/7/1/50>.
- [30] M. Ferro, A. Mannu, W. Panzeri, C.H.J. Theeuwen, A. Mele, An integrated approach to optimizing cellulose mercerization, *Polymers* 12 (2020) 1559, <https://doi.org/10.3390/polym12071559>.
- [31] P.V. Monje, E.J. Baran, Complex biominerization pattern in cactaceae, *J. Plant Physiol.* 161 (1) (2004) 121–123, <https://doi.org/10.1078/0176-1617-01049>.
- [32] P.V. Monje, E.J. Baran, Evidence of formation of glushinskite as a biominerall in a Cactaceae species, *Phytochemistry* 66 (5) (2005) 611–614, <https://doi.org/10.1016/j.phytochem.2004.12.025>.
- [33] P.S. Nobel, *Desert Wisdom/Agaves and Cacti: CO₂, Water, Climate Change, iUniverse*, New York, 2010.
- [34] P. Adamo, P. Violante, Weathering of rocks and neogenesis of minerals associated with lichen activity, *Appl. Clay Sci.* 16 (2000) 229–256, [https://doi.org/10.1016/S0169-1317\(99\)00056-3](https://doi.org/10.1016/S0169-1317(99)00056-3).
- [35] M.J. Wilson, D. Jones, J.D. Russell, Glushinskite, a naturally occurring magnesium oxalate, *Mineral. Magaz.* 1980 (43) (1980) 837–840, <https://doi.org/10.1180/minmag.1980.043.331.02>.
- [36] M.J. Wilson, D. Jones, W.J. McHardy, The weathering of serpentinite by Lecanora atra, *Lichenologist* 198 (13) (1981) 167–176, <https://doi.org/10.1017/S0024282981000212>.
- [37] V.G. Gilev, IR spectra and structure of Si-Al-O-N phases prepared by carbothermal reduction of kaolin in nitriding atmosphere, *Inorg. Mater.* 37 (2001) 1041–1045, <https://doi.org/10.1023/A:1012383211463>.
- [38] E. Robles, J. Fernández-Rodríguez, A.M. Barbosa, O. Gordobil, N.L.V. Carreño, J. Labidi, Production of cellulose nanoparticles from blue agave waste treated with environmentally friendly processes, *Carbohydr. Polym.* 183 (2018) 294–302, <https://doi.org/10.1016/j.carbpol.2018.01.015>.
- [39] V. Babić-Ivančić, H. Füredi-Milhofer, B. Purgarić, N. Brničević, Z. Despotović, Precipitation of calcium oxalates from high ionic strength solutions III. The influence of reactant concentrations on the properties of the precipitates, *J. Cryst. Growth* 71 (3) (1985) 655–663, [https://doi.org/10.1016/0022-0248\(85\)90374-4](https://doi.org/10.1016/0022-0248(85)90374-4).
- [40] N.H. Sulimai, R.A. Rani, Z. Khusaimi, S. Abdullah, M.J. Salifairus, S. Alrokayan, H. Khan, P.A. Sermon, M. Rusop, Facile synthesis of CaCO₃ and investigation on structural and optical properties of high purity crystalline calcite, *Mater. Sci. Eng., B* 243 (2019) 78–85.
- [41] F.A. Andersen, L. Brečević, Infrared spectra of amorphous and crystalline calcium carbonate, *Acta Chem. Scand.* 45 (1991) 1018–1024, <https://doi.org/10.1002/CHIN.199209005>.
- [42] B. Soni, E.B. Hassan, B. Mahmoud, Chemical isolation and characterization of different cellulose nanofibers from cotton stalks, *Carbohydr. Polym.* 134 (2015) 581–589.
- [43] V.S. Yadav, M. Prasad, J. Khan, S.S. Amritphale, M. Singh, C.B. Raju, Sequestration of carbon dioxide (CO₂) using red mud, *J. Hazard. Mater.* 176 (1–3) (2010) 1044–1050.
- [44] J.D. Birchall, J.P. Bellia, N.B. Roberts, On the mechanisms underlying the essentiality of silicon-interactions with aluminium and copper, *Coord. Chem. Rev.* 149 (1996) 231–240, [https://doi.org/10.1016/S0010-8545\(96\)90028-4](https://doi.org/10.1016/S0010-8545(96)90028-4).
- [45] W.R. Taylor, Application of infrared spectroscopy to studies of silicate glass structure: examples from the melilite glasses and the systems Na₂O-SiO₂ and Na₂O-Al₂O₃-SiO₂, *Proc. Indian Acad. Sci.* 99 (1990) 99–117, <https://doi.org/10.1007/BF02871899>.
- [46] U.O. Aroke, A. Abdulkarim, R.O. Ogubunka, Fourier-transform infrared characterization of kaolin, granite, bentonite and barite, *ATBU J. Environ. Technol.* 6 (2013) 42–53.
- [47] A. Morales-Sánchez, J. Barreto, C. Domínguez-Horna, M. Aceves-Mijares, J. A. Luna-López, L. Licea-Jiménez, Silicon Nanoparticles-Based Light Emitting Capacitors, in: H. Li, J. Wu, Z.M. Wand (Eds.), *Silicon-based Nanomaterials*, Springer, New York, 2013, pp. 119–138.
- [48] I.A. Rahman, P. Vejayakumaran, C.S. Sipaut, J. Ismail, C.K. Chee, Size-dependent physicochemical and optical properties of silica nanoparticles, *Mater. Chem. Phys.* 114 (1) (2009) 328–332, <https://doi.org/10.1016/j.matchemphys.2008.09.068>.
- [49] V. Hospodarova, E. Singovszka, N. Stevulova, Characterization of cellulosic fibers by FTIR spectroscopy for their further implementation to building materials, *Am. J. Analyt. Chem.* 9 (6) (2018) 303–310, <https://doi.org/10.4236/ajac.2018.96023>.
- [50] A.M. Efimov, Quantitative IR spectroscopy: applications to studying glass structure and properties, *J. Non-Cryst. Solids* 203 (1996) 1–11, [https://doi.org/10.1016/0022-3093\(96\)00327-4](https://doi.org/10.1016/0022-3093(96)00327-4).
- [51] F.M. Segal, M.F. Correa, R. Bacani, B. Castanheira, M.J. Politi, S. Brochstain, E. R. Triboni, A novel synthesis route of mesoporous γ-alumina from polyoxohydroxide aluminum, *Mater. Res.* 21 (2018), e20170674, <https://doi.org/10.1590/1980-5373-MR-2017-0674>.
- [52] B.W. Liebich, H. Sarp, E. Parthé, The crystal structure of chandalite, CaAl₂(OH)₄SiO₄, *Z. Kristallogr.* 150 (1979) 53–63, <https://doi.org/10.1524/zkri.1979.150.14.53>.
- [53] G. Liang, Y. Li, C. Yang, C. Zi, Y. Zhang, X. Hu, W. Zhao, Production of biosilica nanoparticles from biomass power plant fly ash, *Waste Manage.* 105 (2020) 8–17, <https://doi.org/10.1016/j.wasman.2020.01.033>.